PROCEEDINGS OF SCIENCE

An exploration of Brillouin improvement for Wilson fermions

Stephan Dürr

Universität Wuppertal & Jülich Supercomputing Center, Forschungszentrum Jülich

Giannis Koutsou*

Universität Wuppertal & Jülich Supercomputing Center, Forschungszentrum Jülich

E-mail: i.koutsou@fz-juelich.de

We present a Wilson type operator obtained by adding terms in both the Laplacian as well as the first-derivative stencil, such that the resulting operator remains within a hypercube. Motivated by the effect this improvement has on the eigenvalue spectrum, we carry out a preliminary study of some important features of this operator, such as the approach to the continuum limit of several physical quantities. Throughout we compare to the standard Wilson operator.

The XXVIII International Symposium on Lattice Field Theory, Lattice2010
June 14-19, 2010
Villasimius, Italy

*Speaker.

1. Introduction

The basic operator design of fermion actions used in lattice QCD today, namely Wilson and Susskind type, have changed little since they where first proposed during the seventies. A notable exception are the so called perfect actions [1] which are designed to realize zero cut-off effects as well as exact chiral symmetry, within the scope of the Ginsparg - Wilson relation [2]. Realizing exact chiral symmetry, whether this is achieved using perfect actions or the overlap formulation [3], comes at a huge cost in terms of computer time, usually around two orders of magnitude compared to standard Wilson operators. A more modest approach proposes the modification of the Wilson operator such that chiral symmetry breaking is reduced [4, 5, 6].

In this work we propose a simpler modification, free of tunable parameters, which has a somewhat different target in terms of the desired improvement. We design our operator by investigating various discretizations for the Laplacian as well as the first derivative in the standard Wilson operator. Our choices are motivated by the eigenvalue spectra of these operators, as well as the reduction achieved in rotational symmetry breaking. We test this operator by computing selected hadronic observables, and comparing their approach to the continuum with standard Wilson.

2. Operator construction

The standard Wilson operator can be written as:

$$D(x,y) = \sum_\mu \gamma_\mu \nabla_\mu^{\mathrm{std}}(x,y) - \frac{a}{2}\Delta^{\mathrm{std}}(x,y) + m\delta_{x,y}. \tag{2.1}$$

In the standard case, the first derivative term ($\nabla_\mu^{\mathrm{std}}$), which is forward-backward symmetric, is a 2-point stencil for each direction μ, while the Laplacian (Δ^{std}) is a 9-point stencil in four dimensions. In our approach we add adjacent terms in each positive or negative direction to both operators. Each of the two operators will be at most a 3^d term stencil, d being the number of dimensions. For the off-axis terms, we add all shortest paths of links and then back project to the gauge group.

We will introduce our approach for the simpler case of d=2, and later generalize to d=4 dimensions. In two dimensions, for the case of the Laplacian, we can define the two stencils:

$$\begin{aligned}
\Delta^{\mathrm{std}} &= \boxed{\begin{array}{ccc} 0 & 1 & 0 \\ 1 & -4 & 1 \\ 0 & 1 & 0 \end{array}}\,/1, \quad a^2\hat{\Delta}^{\mathrm{std}}(k_1,k_2) = 2\cos(k_1) + 2\cos(k_2) - 4 \\
\Delta^{\mathrm{til}} &= \boxed{\begin{array}{ccc} 1 & 0 & 1 \\ 0 & -4 & 0 \\ 1 & 0 & 1 \end{array}}\,/2, \quad a^2\hat{\Delta}^{\mathrm{til}}(k_1,k_2) = 2\cos(k_1)\cos(k_2) - 2
\end{aligned} \tag{2.2}$$

which we name the standard and tilted Laplacians respectively. In Eq. (2.2) we additionally show the corresponding operators in Fourier space. By taking the linear combination $\alpha\Delta^{\mathrm{std}} + (1-\alpha)\Delta^{\mathrm{til}}$ we can choose α such that the resulting Laplacian has certain desirable properties. Two such choices of α are most notable, namely $\alpha = 1/2$ and $\alpha = 2/3$. The choice $\alpha = 1/2$ will be referred to as the Brillouin Laplacian, and is notable for the fact that it takes on a constant value on the entire boundary of the Brillouin zone. The choice $\alpha = 2/3$ will be referred to as the Isotropic Laplacian, and has the property that in Fourier space, for small momenta, it depends only on the combination $k_1^2 + k_2^2$ up to and including $O(a^4)$. In other words, deviation from the continuum is isotropic, i.e. it is the same whether on- or off-axis, for small momenta, up to this order. The stencils as well as their Fourier space representations are given below:

$$
\begin{aligned}
\Delta^{\text{bri}} &= \boxed{\begin{array}{ccc} 1 & 2 & 1 \\ 2 & \text{-12} & 2 \\ 1 & 2 & 1 \end{array}}\,/4, \quad a^2\hat{\Delta}^{\text{bri}}(k_1,k_2) = 4\cos^2(k_1/2)\cos^2(k_2/2) - 4 \\
\Delta^{\text{iso}} &= \boxed{\begin{array}{ccc} 1 & 4 & 1 \\ 4 & \text{-20} & 4 \\ 1 & 4 & 1 \end{array}}\,/6, \quad a^2\hat{\Delta}^{\text{iso}}(k_1,k_2) = [2\cos(k_1)\cos(k_2) + 4\cos(k_1) + 4\cos(k_2) - 10]/3
\end{aligned}
\tag{2.3}
$$

Similarly, one can define Brillouin and Isotropic stencils for the case of the first derivative. The stencils corresponding to a single direction, along with their expressions in Fourier space, are given below:

$$
\begin{aligned}
\nabla_x^{\text{bri}} &= \boxed{\begin{array}{ccc} \text{-1} & 0 & 1 \\ \text{-2} & 0 & 2 \\ \text{-1} & 0 & 1 \end{array}}\,/8, \quad a\hat{\nabla}_{\hat{x}}^{\text{bri}} = i\sin(k_1)[\cos(k_2) + 1]/2 \\
\nabla_x^{\text{iso}} &= \boxed{\begin{array}{ccc} \text{-1} & 0 & 1 \\ \text{-4} & 0 & 4 \\ \text{-1} & 0 & 1 \end{array}}\,/12, \quad a\hat{\nabla}_{\hat{x}}^{\text{iso}} = i\sin(k_1)[\cos(k_2) + 2]/3
\end{aligned}
\tag{2.4}
$$

We construct our improved operators by taking combinations between these choices of first derivatives and Laplacians. We investigate the eigenvalue spectra to qualitatively identify the features of each combination. In Fig. 1 we show the spectra for all combinations of Laplacian and first derivative when considering the three discretizations (Standard, Brillouin and Isotropic) for each operator.

Our final choice is to use the Isotropic first derivative in combination with the Brillouin Laplacian. We are motivated to choose this specific combination since we expect a reduction in the condition number of the operator when compared to standard Wilson, mainly due to the fact that the Brillouin Laplacian lifts the doublers by the same amount. This is particularly important when the operator is used as a kernel for the overlap operator. In addition we expect less rotational symmetry violation as compared to the standard Wilson operator.

Generalizing the above to four dimensions is beyond the purpose of this proceedings contribution. However, in Eq. (2.5) we present the stencils of the Isotropic derivative and Brillouin Laplacian, which we will use throughout this contribution, and hereafter refer to as the Brillouin improved operator. In Fig. 2 we compare the eigenvalue spectra of the Brillouin improved operator with that of standard Wilson on U(1) backgrounds, in two dimensions as well as four dimensions.

PoS(Lattice 2010)087

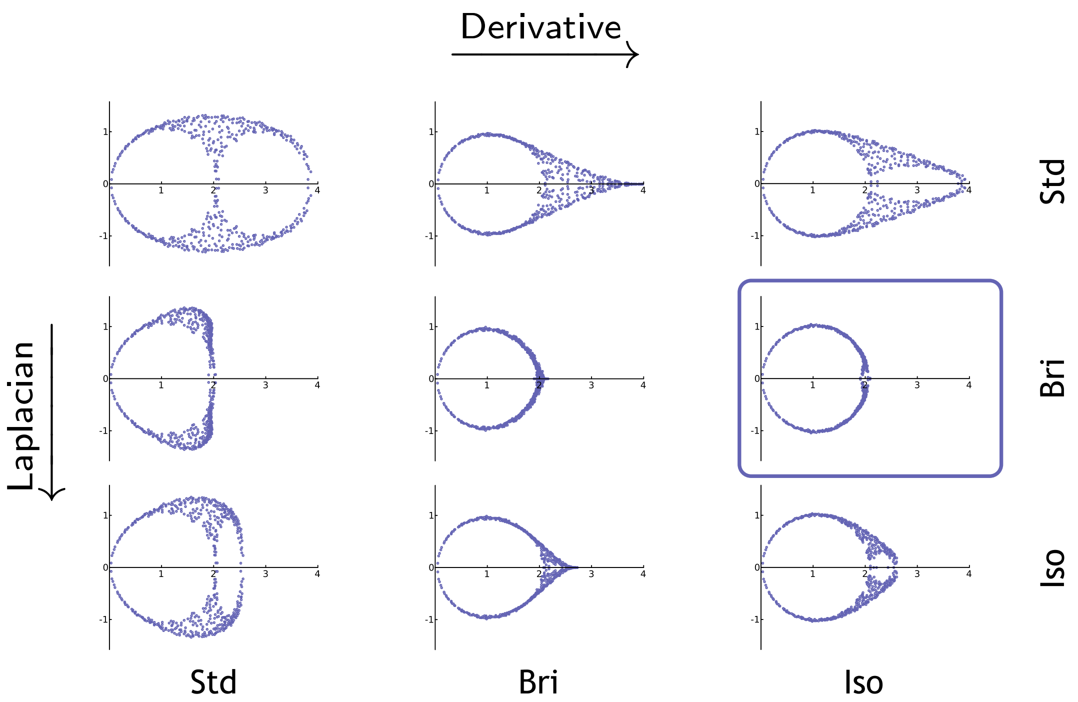

Figure 1: Eigenvalue spectra of the fermion operator for all combinations of first derivative and Laplacian discretizations. The spectra where obtained on a 16×16 U(1) gauge field, using clover improvement with c_{SW} = 1. The framed spectrum corresponds to our choice, to which we refer to as the Brillouin operator.

$$\nabla_x^{\rm iso} = \begin{array}{|ccc|ccc|ccc|}\hline -1 & 0 & 1 & -4 & 0 & 4 & -1 & 0 & 1 \\ -4 & 0 & 4 & -16 & 0 & 16 & -4 & 0 & 4 \\ -1 & 0 & 1 & -4 & 0 & 4 & -1 & 0 & 1 \\ \hline -4 & 0 & 4 & -16 & 0 & 16 & -4 & 0 & 4 \\ -16 & 0 & 16 & -64 & 0 & 64 & -16 & 0 & 16 \\ -4 & 0 & 4 & -16 & 0 & 16 & -4 & 0 & 4 \\ \hline -1 & 0 & 1 & -4 & 0 & 4 & -1 & 0 & 1 \\ -4 & 0 & 4 & -16 & 0 & 16 & -4 & 0 & 4 \\ -1 & 0 & 1 & -4 & 0 & 4 & -1 & 0 & 1 \\ \hline \end{array} /432 \qquad \Delta^{\rm bri} = \begin{array}{|ccc|ccc|ccc|}\hline 1 & 2 & 1 & 2 & 4 & 2 & 1 & 2 & 1 \\ 2 & 4 & 2 & 4 & 8 & 4 & 2 & 4 & 2 \\ 1 & 2 & 1 & 2 & 4 & 2 & 1 & 2 & 1 \\ \hline 2 & 4 & 2 & 4 & 8 & 4 & 2 & 4 & 2 \\ 4 & 8 & 4 & 8 & -240 & 8 & 4 & 8 & 4 \\ 2 & 4 & 2 & 4 & 8 & 4 & 2 & 4 & 2 \\ \hline 1 & 2 & 1 & 2 & 4 & 2 & 1 & 2 & 1 \\ 2 & 4 & 2 & 4 & 8 & 4 & 2 & 4 & 2 \\ 1 & 2 & 1 & 2 & 4 & 2 & 1 & 2 & 1 \\ \hline \end{array} /64 \tag{2.5}$$

3. Practical Tests

We carry out a number of tests in 4D to compare our Brillouin operator with the standard Wilson case. We use five ensembles of quenched SU(3) Wilson lattices at a fixed box size of around ~ 1.5 fm. Details of the ensembles are listed in Tab. 1. For all tests we use one step of APE smearing [7], with the weight chosen at $\alpha_{\rm APE} = 0.72$.

In Fig. 3 we compare the convergence history of inverting either operator using the BiCGStab algorithm on the same configuration. We have tuned such that the two inversions correspond to the same quark mass. From the plot it is apparent that the Brillouin improved operator converges at around half the iterations required in the standard Wilson case. Taking into account the computational cost of a single application of the Brillouin improved operator, we conclude that an inversion using our improved operator is around 10 times more expensive than using standard Wilson.

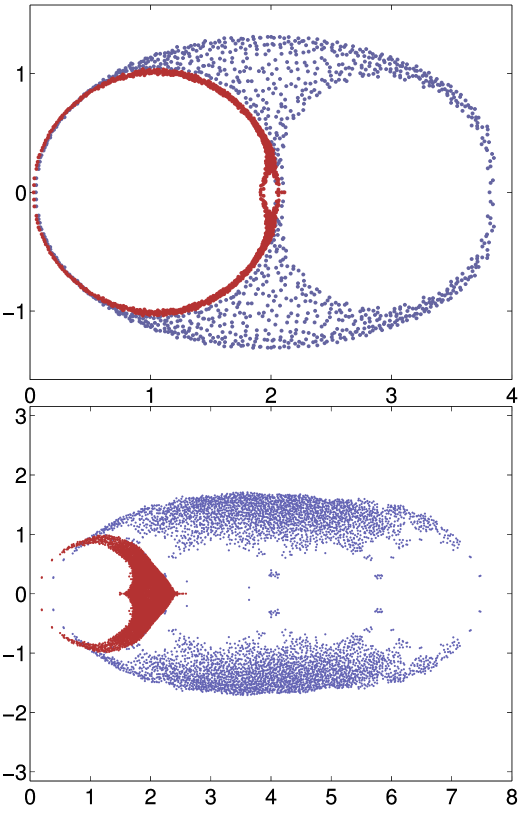

Figure 2: Comparison of the eigenvalue spectra of the standard Wilson operator (blue) and the Brillouin improved operator (red), in two dimensions (top) and four dimensions (bottom), on U(1) backgrounds with $c_{SW} = 1$.

Table 1: The quenched SU(3) configuration ensembles used for our tests.

size	β	a (fm)	a^{-1} (GeV)
$10^3 \times 20$	5.72	0.160	1.236
$12^3 \times 24$	5.80	0.133	1.479
$16^3 \times 32$	5.95	0.100	1.978
$20^3 \times 40$	6.08	0.080	2.463
$24^3 \times 48$	6.20	0.067	2.964

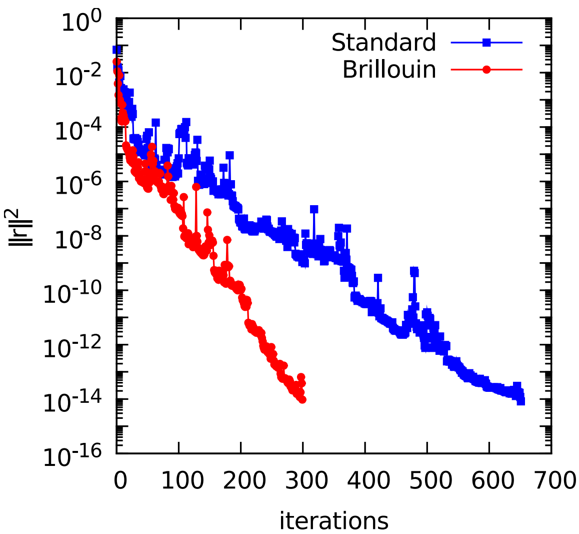

Figure 3: Convergence history of BiCGStab for the standard Wilson case (blue) and the Brillouin improved operator (red).

In order to carry out scaling tests we need to compare the two operators at the same physical pion mass. Thus we carry out tuning runs where we scan for several values of the bare quark mass and measure the effective mass of the pseudoscalar meson. This tuning is shown in Fig. 4, where we plot the square of the pseudoscalar meson mass as a function of the inverse hopping parameter, in units of the Sommer scale (r_0). The solid horizontal lines correspond to two values of the pseudoscalar mass which we explicitly target, in order to carry out the scaling tests, namely $(r_0 M_P)^2 = 1.56$ and $(r_0 M_P)^2 = 4.56$, which we will hereby refer to as "light" and "strange". We additionally tune for a "charm" quark mass to yield $(r_0 M_P)^2 = 46.5$.

In Fig. 5 we plot the bare quark mass as a function of the bare coupling (g_0), for the two aforementioned values of $r_0 M_P$, as well as for $r_0 M_P = 0$ (the critical bare mass). The dashed lines are fits to a rational ansatz: $\frac{c_1 g_0^2 + c_2 g_0^2}{1 + c_3 g_0^2}$.

Having Fig. 5 we know exactly which bare quark mass to dial at any given lattice spacing for the three target pseudoscalar meson masses. We confirm this in Fig. 6 where we plot the masses of the pion, kaon and pseudoscalar $s\bar{s}$ as a function of the lattice spacing squared. Having confirmed that both operators have been tuned to the same mass at all spacings, we go on to compare the approach to the continuum of the nucleon mass and the cascade mass using the two operators. The comparison is shown in Fig. 7, where we see that up to the coarsest lattice there is no significant difference between the values obtained by the two operators.

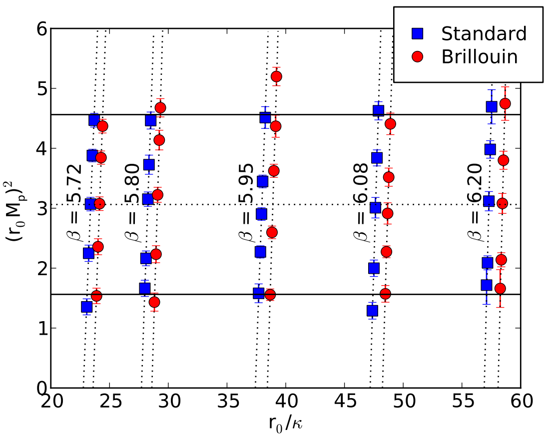

Figure 4: Tuning of pseudoscalar meson masses for both operators.

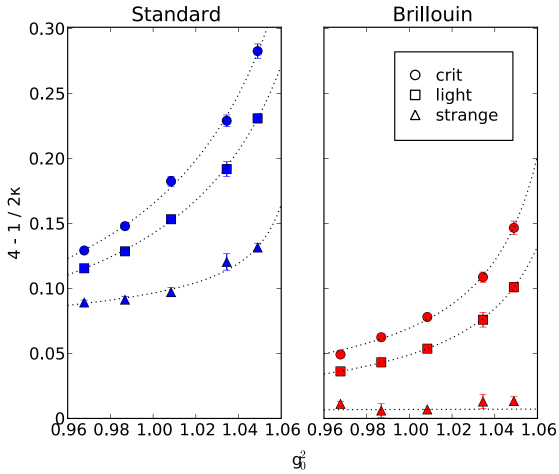

Figure 5: Plot of the bare mass parameter, corresponding to a given pseudoscalar mass, as a function of the bare coupling.

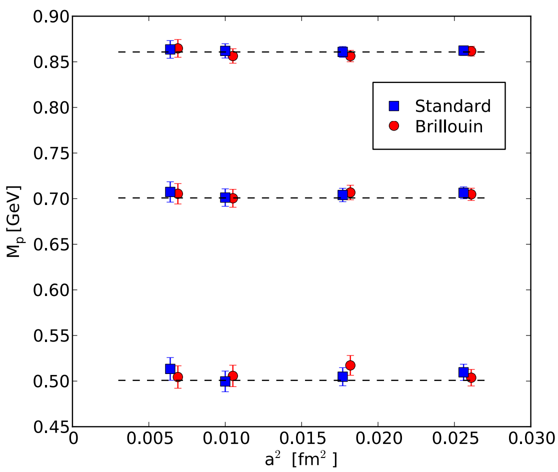

Figure 6: Pion, kaon and $\bar{s}s$ meson masses as a function of the lattice spacing squared.

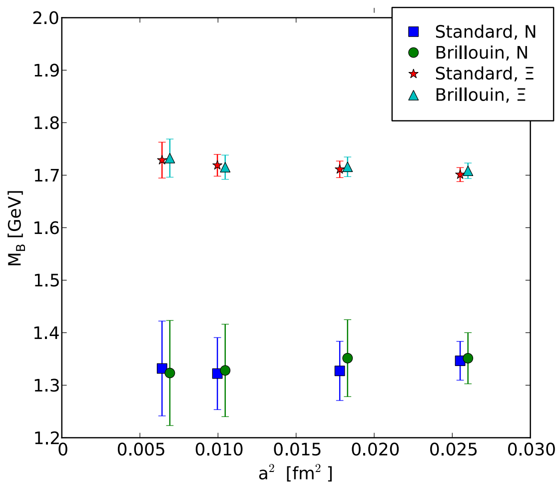

Figure 7: Nucleon and cascade masses for both operators at all lattice spacings.

In Fig. 8 we show ratios of unimproved decay constants of pseudoscalar mesons for two cases: the pseudoscalar strange over the pion decay constant and the pseudoscalar charm over the pseudoscalar strange decay constant. The ratios are taken in order to eliminate the unknown axial current renormalization constant Z_A, and thus compare directly the standard Wilson operator with the Brillouin improved operator. As can be seen, for $f_{\bar{s}s}/f_{\bar{l}l}$, there seems to be no significant difference between the two operators, and the continuum extrapolation appears to be flat within error bars. For the other case of $f_{\bar{c}c}/f_{\bar{s}s}$ we see a significant difference. It appears that the scaling region for the case of the Brillouin improved operator extends further than that of standard Wilson. This is an indication that cut-off effects may be more regularly behaved for the Brillouin improved operator, since these are expected to be more pronounced for observables of heavy quarks.

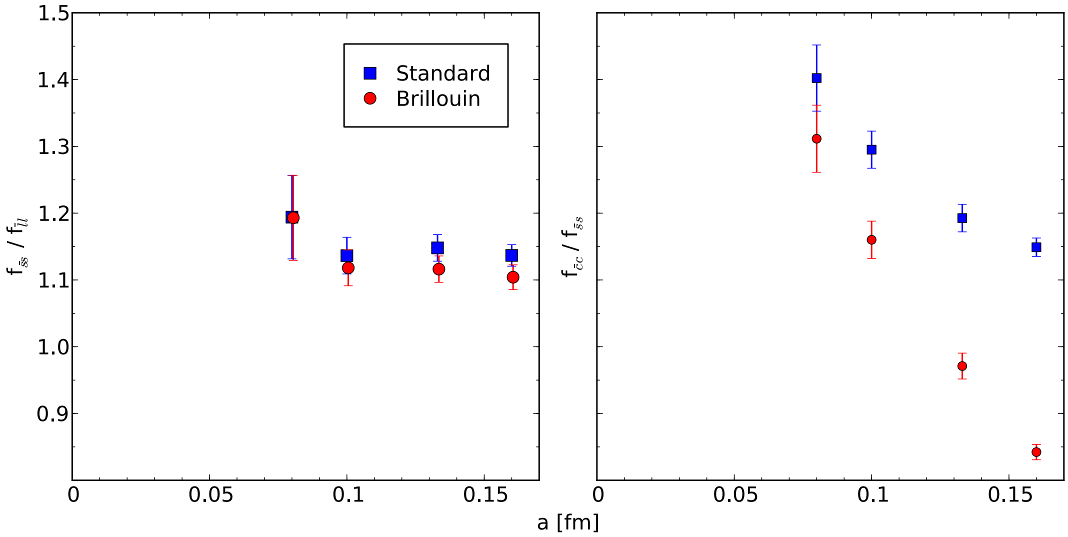

Figure 8: Ratio of meson decay constants as a function of the lattice spacing. Left for $s\bar{s}$ over the pion, and right for $c\bar{c}$ over $s\bar{s}$.

4. Conclusions and Summary

In this contribution, we have presented a new method for improvement of Wilson fermions and have carried out a preliminary investigation on the operator this improvement yields. This preliminary investigation shows that this operator is approximately ten times more expensive to invert than standard Wilson. It is yet to be fully determined whether this increased computational cost pays off at the end. So far our tests show that for the Brillouin operator the scaling region may be larger, extending to coarser lattice spacings for the case of observables involving heavy quarks, as compared to standard Wilson.

Another aspect we hope to clarify is the suitability of this improved operator as a kernel for the overlap operator. The eigenvalue spectra suggest that using our method, the shifted operator $A = D^{\dagger}_{-1}D_{-1}$ has a smaller condition number than that of standard Wilson. A calculation of the dependence of the smallest and largest eigenvalues on the bare mass will shed light on this subject.

Acknowledgments: Computations where carried out on the Juropa cluster through a NIC grant.

References

[1] P. Hasenfratz and F. Niedermayer *Nucl. Phys.* **B414** (1994) 785–814, [hep-lat/9308004] .

[2] P. H. Ginsparg and K. G. Wilson *Phys. Rev.* **D25** (1982) 2649 .

[3] H. Neuberger *Phys. Lett.* **B417** (1998) 141–144, [hep-lat/9707022] .

[4] W. Bietenholz, R. Brower, S. Chandrasekharan, and U. J. Wiese *Nucl. Phys. Proc. Suppl.* **53** (1997) 921–934, [hep-lat/9608068] .

[5] **MILC** Collaboration, T. A. DeGrand *Phys. Rev.* **D58** (1998) 094503, [hep-lat/9802012] .

[6] C. Gattringer *Phys. Rev.* **D63** (2001) 114501, [hep-lat/0003005] .

[7] **APE** Collaboration, M. Albanese *et. al. Phys. Lett.* **B192** (1987) 163–169 .